

# Diamond cylindrical anodes for electrochemical treatment of persistent compounds in aqueous solution

Hudson Zanin · Reinaldo F. Teófilo · Alfredo C. Peterlevitz ·  
Ulisses Oliveira · Juliana C. de Paiva · Helder José Ceragioli ·  
Efraim L. Reis · Vitor Baranauskas

Received: 25 July 2012 / Accepted: 8 October 2012 / Published online: 21 October 2012  
© Springer Science+Business Media Dordrecht 2012

**Abstract** Boron-doped diamond (BDD) films were deposited onto either silicon or niobium cylindrical substrates with areas up to 35 cm<sup>2</sup> for electrochemical applications. BDD electrodes were characterised in terms of their material and electrochemical properties by scanning electron microscopy, Raman spectroscopy and linear sweep voltammetry. These characterisation techniques indicated conductive polycrystalline BDD with low quantities of non-diamond carbon impurities. Electrochemical oxidations of pharmaceutical compounds were performed using these cylindrical electrodes and monitored by UV/Vis spectroscopy, chemical oxygen demand and total organic carbon. Mixtures of chlortetracycline, oxytetracycline and diclofenac were electrolyzed on a 9.42 cm<sup>2</sup> ( $\varnothing = 6$  mm,  $h = 50$  mm) cylindrical Si/BDD anode using a current density of 8.2 mA cm<sup>-2</sup>. Ibuprofen was electrolyzed on an 18.0 cm<sup>2</sup> ( $\varnothing = 10$  mm,  $h = 60$  mm) cylindrical Nb/BDD anode using a current density of 25 mA cm<sup>-2</sup>. Cylindrical-shape diamond electrodes present several advantages with respect to conventional plate-shape BDD electrodes such as handling, sealing and cell assembly. The obtained results show that BDD cylindrical anodes are promising for electrochemical wastewater treatment.

**Keywords** Cylindrical diamond electrode · BDD · Diamond anode · Electrochemical oxidation · Micro-pollutants · Chemical vapour deposition

## 1 Introduction

One environmental problem facing humanity is the increasing pollution of freshwater systems by chemically active substances [1]. Many studies have documented the presence of drugs, pesticides, dyes and many other toxic compounds in rivers, lakes, groundwater and other sources of water [1–3]. Some of these pollutants are persistent in conventional drinking-water treatments (DWT), causing considerable toxicological concern, particularly when they form complex mixtures [1–4].

According to Schwarzenbach et al. [1], there are three challenges that must be met: (i) development of new methodologies to assess the impact of these pollutants on aquatic life and human health (ii) minimization of the introduction of critical pollutants into the aquatic system through more environmentally healthy products and processes, and (iii) the new cost-effective and appropriate remediation of water-treatment technologies.

Advanced oxidation processes (AOP) have been studied to degrade recalcitrant compounds in water. However, the by-products generated by AOP may cause more serious problems for human health and the environment [5, 6]. The selection of treatment depends on the optimal control, reliability, cost-effectiveness and efficiency (oxidative and economic) being considered. Electrochemical oxidation is considered one of the most promising techniques for wastewater treatment [7–11].

H. Zanin · A. C. Peterlevitz · H. J. Ceragioli · V. Baranauskas  
Departamento de Semicondutores, Instrumentos e Fotônica,  
Faculdade de Engenharia Elétrica e de Computação,  
Universidade Estadual de Campinas, Campinas, SP 13083-852,  
Brazil

R. F. Teófilo (✉) · U. Oliveira · J. C. de Paiva · E. L. Reis  
Departamento de Química, Universidade Federal de Viçosa,  
Viçosa, MG 36570-000, Brazil  
e-mail: rteofilo@gmail.com

Many investigations have been conducted employing electrodes of different materials such as Pt, Carbon, boron-doped diamond (BDD) and metal oxides such as  $\text{RuO}_2$ ,  $\text{PbO}_2$ ,  $\text{IrO}_2$  and  $\text{SnO}_2$ , which are used as anodes for the degradation of organic and inorganic pollutants [12–14]. Among them, the results obtained for depollution with  $\text{PbO}_2$  and BDD are especially notable; however, BDD is more reactive than  $\text{PbO}_2$ , leading to remarkably higher current efficiency and lower specific-energy consumption [14]. Over the past decades, boron-doped diamond (BDD) electrodes prepared by the CVD process have been used successfully for the treatment of wastewater containing persistent compounds. These electrodes have shown higher efficiency as electrochemical systems for the same purpose [7, 14–16].

BDD electrodes have been prepared on plates or wire-shaped substrates of various materials with areas up to  $50 \times 60$  and  $1.8 \text{ cm}^2$ , respectively, as reported in the literature [17–22]. Even though a variety of materials have already been tested for diamond CVD deposition, the most used substrate is still p-type silicon wafer, which is usually too much brittle, limiting its large-scale production. Conventional electrochemical cells that use plate-shaped electrodes present difficulties with: (i) sealing and hydraulic connections; (ii) making high quality and impermeable electrical contacts; (iii) assembly of parts [23].

To the best of our knowledge, BDD electrodes have only been prepared onto plate and wire-shaped substrates for electrochemical degradation. By contrast, our research group has prepared BDD electrodes on cylindrical-shaped substrates with a diameter greater than 2 mm [23, 24]. This article presents applications of these cylindrical electrodes for electrochemical degradation.

Cylindrical-shaped (rod and tube substrates) electrodes are promising for: (i) making suitable sealing and hydraulic connections without the need to use resins or adhesives; (ii) facilitating handling; (iii) facilitating large-scale assembly connections in series and/or in parallel; (iv) making high quality electrical contacts, and (v) minimizing physical size [23].

This study presents the deposition of BDD films onto different cylindrical substrates of different materials, i.e., silicon (Si) and niobium (Nb). Morphological characterisation was performed with scanning electron microscopy (SEM); structural characterisation was done by Raman spectroscopy and electrochemical characterisation was carried out by linear sweep voltammetry. Subsequently, the BDD electrodes were applied for electrochemical degradation of pharmaceutical compounds. The electrochemical oxidation was monitored using UV/Visible spectroscopy, chemical oxygen demand (COD) and total organic carbon (TOC).

## 2 Experimental

### 2.1 Chemicals

Ibuprofen (Ibu), chlortetracycline hydrochloride, oxytetracycline hydrochloride and diclofenac sodium (analytical grade powder, >99 % pure) were purchased from Sigma-Aldrich (U.S.A). Boron trioxide (analytical grade powder, >99 % pure) was purchased from Merck (Germany). Ethanol and  $\text{Na}_2\text{SO}_4$  was provided by Vetec (Brazil) with purity 98 %. Solutions of pharmaceuticals were prepared with Milli-Q purified water in the presence of supporting  $\text{Na}_2\text{SO}_4$  electrolyte. All chemicals were used without further purification.

### 2.2 Preparation of electrodes

Diamond films were deposited onto rods of silicon ( $\varnothing = 6 \text{ mm}$ ,  $h = 110 \text{ mm}$ ) and niobium ( $\varnothing = 10 \text{ mm}$ ,  $h = 110 \text{ mm}$ ) using a hot-filament-assisted chemical vapour deposition system (HFCVD). Two different cylindrical substrates and two different diameters were studied to show the applicability and possibilities of this shape as an electrode in electrochemical degradation. Prior to deposition, the substrates were pre-treated by sand blasting, following by cleaning techniques and subsequently immersed in a mixture of 10 mL of castor oil and 1 mg of diamond powder.

The substrate and two vertical straight filaments were positioned face-to-face, parallel to the gas flux, inside the reactor chamber. A mixture of ethanol ( $\text{C}_2\text{H}_5\text{OH}$ ), water and boron trioxide in hydrogen (90 % vol) was used as the HFCVD feedstock. The system works with a total flow rate of approximately 100 sccm and at a total pressure of  $\sim 20$  Torr. During the deposition process, the substrates were rotated at approximately 4 rpm by magnetic coupling to an electric motor outside the reactor chamber. The filaments were kept flat by mechanical compensation to stretch them [24].

In all the experiments, tungsten filaments 272  $\mu\text{m}$  in diameter and 120 mm in length were electrically fed with 610 W of constant power. The deposition processes were automated using a programmable control unit. The temperature was gradually raised to the desired value and, after the deposition period, the cooling was very slow. The growth rates were 1.5 and 3  $\mu\text{m h}^{-1}$  for the deposition onto Si and Nb, respectively. The thickness was about 90  $\mu\text{m}$  (deposition time 60 h) and 24  $\mu\text{m}$  (deposition time 8 h) for Si and Nb, respectively.

### 2.3 Electrode characterisation

Morphological images were performed using a field emission scanning electron microscope (FESEM, JEOL

JSM-6330F equipment) operating at an accelerating voltage of 5 kV and a beam current of 8  $\mu\text{A}$ .

Raman spectra were recorded at room temperature using a Renishaw InVia Raman spectroscopy microprobe system with blue laser excitation (488 nm) at a laser power of approximately 6 mW.

Voltammetric analyses were carried out to determine the potential window of the BDD films. The Si/BDD and Nb/BDD were used as working electrodes; Ag/AgCl and platinum wire were used as the reference electrode and counter electrode, respectively. The geometric area of the work electrodes was about 0.2 cm<sup>2</sup>. Linear sweep voltammetry was applied in the range of  $-1.5$  to  $3.0$  V. The scan was performed in 2 mol L<sup>-1</sup> H<sub>2</sub>SO<sub>4</sub> solution. In all the experiments, a potentiostat–galvanostat Eco Chimie Autolab PGSTAT10 was used.

## 2.4 Bulk electrolysis

Bulk electrolysis was performed under galvanostatic conditions at room temperature (25 °C) in a beaker equipped with two electrodes (Fig. 1). BDD was used as the anode, with an exposed geometric area of 9.42 cm<sup>2</sup> ( $\varnothing = 6$  mm,  $h = 50$  mm) and 18.0 cm<sup>2</sup> ( $\varnothing = 10$  mm,  $h = 60$  mm) for electrodes prepared with Si and Nb, respectively. Two connected stainless steel concave-convex plates were used as cathodes. The plates were placed face-to-face with the central cylindrical anode. The gap between each cathode and anode was about 5 mm and the current density was kept constant at 8.2 and 25 mA cm<sup>-2</sup> for Si/BDD and Nb/BDD, respectively. As the supporting electrolyte, 5 g L<sup>-1</sup> of Na<sub>2</sub>SO<sub>4</sub> was introduced into the initial electrochemical system.

The electrolytic volume system was continuously stirred by a magnetic bar throughout the process. Samples were collected from the cell at prescribed intervals for chemical and spectral analysis. Before the experiments the BDD electrode was washed with deionized water. A blank control with only 5 g L<sup>-1</sup> Na<sub>2</sub>SO<sub>4</sub> in 250 mL solution was prepared for each electrolysis test. Solutions of ibuprofen 50 mg L<sup>-1</sup> and a mixture of pharmaceutical compounds i.e., chlortetracycline chloride 186.67 mg L<sup>-1</sup>, oxytetracycline chloride 186.67 mg L<sup>-1</sup> and diclofenac sodium 186.67 mg L<sup>-1</sup>, totalling 560.00 mg L<sup>-1</sup> were electrolyzed. Higher concentrations than those found in sewage treatment plants and natural effluents were chosen to better evaluate the oxidative ability of the cylindrical BDD anodes. The volume and time used for each electrolysis test were, respectively: 500 mL and 10 h for Si/BDD application and 250 mL and 5 h for Nb/BDD application.

## 2.5 Analytical methods

The total organic carbon (TOC) was obtained on a total organic carbon analyser Shimadzu TOC 5000A (LOD = 4  $\mu\text{g L}^{-1}$ ).

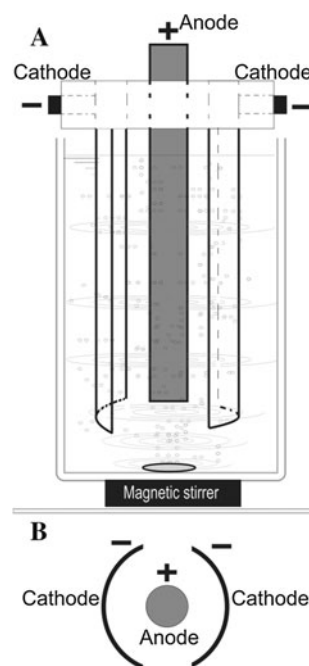


**Fig. 1** **a** Side view of the scheme of electro-degradation experimental setup. The cylindrical BDD electrode is designated as anode (+). Two concave-convex electrodes of stainless steel (AISI304) are designated as cathodes (-). The treated solutions were stirred using magnetic stirrer. **b** Top view of the electrodes

Chemical oxygen demand (COD) was performed according to Li et al. [25] and the spectra and COD readings were obtained using a spectrograph UV/Vis USB-4000 connected to a source DH-2000-BAL from Ocean Optics (USA).

## 3 Results and discussion

### 3.1 SEM and Raman characterization

Figure 2a, b shows typical micrographs obtained by scanning electron microscopy (SEM) of as-deposited diamond films onto Si and Nb, respectively. It can be observed that the polycrystalline diamond films mainly exhibit pyramidal grain shapes with edges wider than 1  $\mu\text{m}$ .

Due to the continuous rotation of the substrate during growth, the diamond films have excellent homogeneity over the entire area. Moreover, irrespective of the substrate material (silicon or niobium), the diamond films have similar micro-morphology with the same experimental parameters [18, 21, 26, 27]. Inhomogeneous topography is always observed in both cases, originating from the increased substrate surface roughness, due to the sand-blasted surface.

Typically, no delamination or cracks were identified in the diamond films deposited onto sand-blasted substrates.

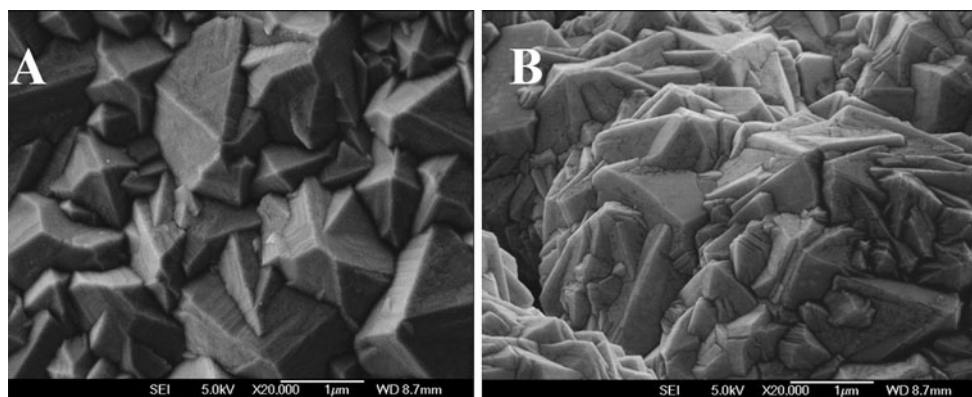
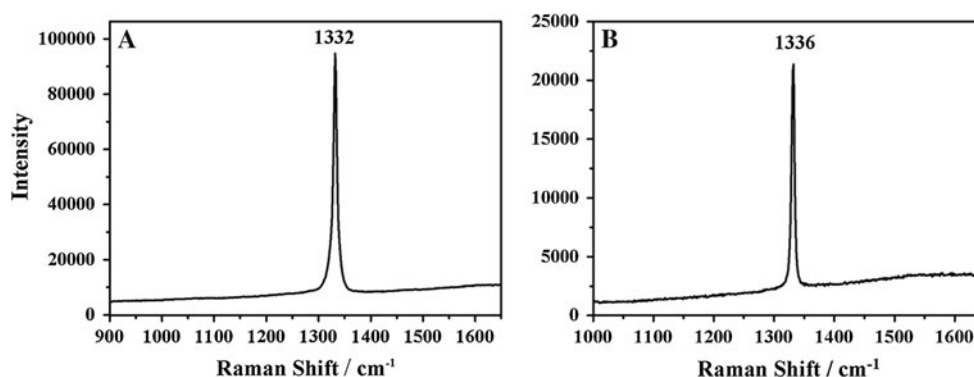


**Fig. 2** Typical micro-morphologies of as-deposited diamond on rods of **a** silicon and **b** niobium substrates

**Fig. 3** Typical Raman spectra from as-deposited diamond films on rods of **a** silicon and **b** niobium substrates



Improved adherence and minimization of cracks in the diamond films were observed on substrates with rougher surfaces, which is in agreement with Fryda et al. [28].

Figure 3a, b shows typical Raman spectra of as-deposited diamond films onto Si and Nb substrates, respectively. High quality diamond films are observed in both cases with almost no graphitic phase detection. The occurrence of intense first-order Raman peaks at  $1,332\text{ cm}^{-1}$  was typically observed on films prepared onto Si substrates, indicating that there is no residual stress in the film. However, the Raman shift peak position is  $1,336\text{ cm}^{-1}$  for diamond prepared onto Nb substrates, indicating that compressive stress is predominant. The extrinsic stress, originating from the different thermal expansion coefficients between the materials (coatings and substrates), is the reason for the typical shift up in the diamond peak's position.

Overall, it was observed that the SEM images and the Raman spectra show enough diamond quality to be applied to electro-degradation and also do not have characteristics different from typical diamond reported elsewhere [18, 29–31].

### 3.2 Voltammetric measurements

Background voltammograms can be very informative about diamond quality and electrical conductivity

[18, 29, 32]. The presence of non-diamond carbon impurities at the surface can be detected from the background voltammogram in a strong acid media, especially by virtue of its effect on the width of the potential domain, where the electrode is ideally polarizable [18, 29]. The background for Si/BDD (Fig. 3a) and Nb/BDD (Fig. 3b) electrodes is featureless, low and ideally polarizable in their respective potential ranges from  $-380$  to  $1,056\text{ mV}$  and from  $-420$  to  $1,360\text{ mV}$  in  $2.0\text{ mol L}^{-1}\text{ H}_2\text{SO}_4$ , as can be seen in Fig. 4. Oxygen evolution at the BDD was estimated to start at about  $1.5$  and  $1.9\text{ V}$  versus Ag/AgCl on Si/BDD and Nb/BDD, respectively. At these potentials, oxidation of water and formation of hydroxyl radicals on the BDD electrode occurs [33].

The exposed geometric area was  $0.94\text{ cm}^2$  for both electrodes and all currents were normalized to this area. The potential window can be related, in part, to the lower fraction of exposed grain boundaries [18, 29, 30]. The electrodes were seen to have a similar potential window, presenting a lower fraction of exposed grain boundaries, which is in agreement with the literature [18, 29, 30]. The voltammograms also indicate that no significant level of non-diamond carbon impurities is present. From the inner plot in Fig. 4, it can be seen that the density current for Si/BDD is lower than for Nb/BDD due to the better conductivity of niobium. The



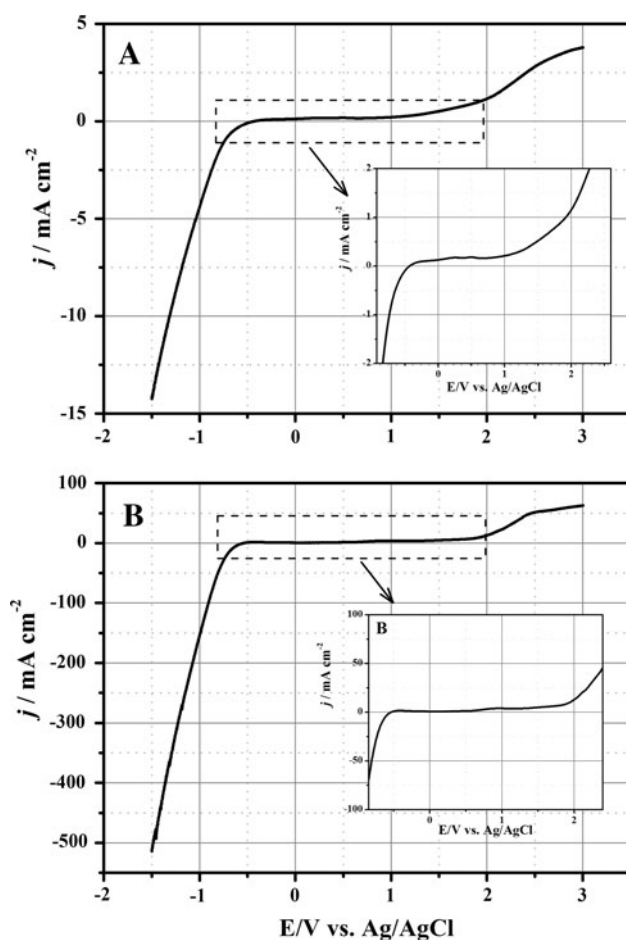


**Fig. 4** Background linear sweep voltammograms performed in  $\text{H}_2\text{SO}_4$  solution  $2 \text{ mol L}^{-1}$  for **a** Si/BDD and **b** Nb/BDD

voltammograms show that the diamond has enough quality to be applied to electro-degradation and also does not have the different characteristics of voltammograms obtained on plates or wafers [17, 29, 34, 35].

### 3.3 Electrochemical degradation of pharmaceutical compounds

A simulated aqueous solution of pharmaceuticals was prepared and electrolyzed using the cylindrical anodes coated with BDD films. Ibuprofen, chlortetracycline hydrochloride, oxytetracycline hydrochloride and diclofenac sodium were chosen because these drugs have been found in domestic wastewater (sewage) and in conventional drinking-water treatment plant facilities, but at lower concentrations than those studied in this study [36–41]. Ibuprofen and diclofenac have been electrolyzed in previous works [42–47], but electrochemical degradation studies of pharmaceutical drug mixtures were not found in the literature. The aim of this electro-oxidation study was to present the application of cylindrical anodes as a feasible

and promising geometric-shape with respect to plates for wastewater treatment.

Figure 5 shows the electro-oxidation of the pharmaceutical mixture using the Si/BDD anode. Fig. 5a presents the UV/Vis spectra obtained during the process. Notice that all compounds and their by-products present absorbance between about 240 and 400 nm. Absorbance in this range emphasizes the strong chemical bonds of the compounds presents in the mixture. The pure absorption spectra of tetracyclines in water were characterized by two major absorption bands at 276 and 358 nm; these bands continued into the tetracycline degradation. The spectrum of diclofenac, which has a maximum at 274 nm, did not significantly contribute to the spectrum of the mixture [47, 48]. The peaks at 276 and 358 nm decreased with the electrolysis time in accordance with Rossi et al. and Zhang et al. [48, 49].

Despite this, absorbance removing was acceptable, considering the results shown in Fig. 5b. The norm absorbance presented in Fig. 5b considers the information from the full spectrum and is calculated using the following equation  $\| \text{Absorbance} \| = \sqrt{x^t x}$ , where  $x$  is a defined spectrum. The absorbance removal norm was about 60 %.

Pharmaceutical mixture removal was monitored using TOC and COD and is presented in Fig. 5c. Satisfactory removals were 58 and 48 %, respectively, for TOC and COD after  $1.7 \text{ h L}^{-1}$  on the Si/BDD anode, reaching an energy efficiency of  $5.76 \text{ kWh m}^{-3}$ .

Electro-oxidation of oxytetracycline and tetracycline has been performed in previous works using  $\text{RuO}_2$  and  $\text{Ti/RuO}_2\text{--IrO}_2$  electrodes [48, 49], but no results about the organic matter removal were presented. However, the results of Rossi et al. (2009) showed that the process minimized the antibiotics' effectiveness against *Staphylococcus aureus* bacteria.

With respect to diclofenac, Ciríaco et al. [46] oxidized this molecule on a  $\text{Ti/SnO}_2\text{--Sb}_2\text{O}_4$  anode, removing 73 % of TOC after 24 h at  $20 \text{ mA cm}^{-2}$ . Zhao et al. [50] monitored diclofenac degradation on a BDD electrode using HPLC–DAD and found a 72 % removal of the diclofenac molecule after 4 h. However, the removal of TOC and COD was not monitored. Brillas et al. [45] incinerated diclofenac in neutral aqueous medium by anodic oxidation using Pt and BDD. Pt gave poor decontamination. BDD achieved 73 % mineralization in 6 h.

Our results indicated significant efficiency in the removal of a mixture containing antibiotics and diclofenac. Thus, the cylindrical shape appears not to have affected the performance of the anode.

Figure 6 shows the electro-oxidation of ibuprofen using a cylindrical Nb/BDD anode in  $\text{Na}_2\text{SO}_4$  solution at  $25 \text{ mA cm}^{-2}$ . Ibuprofen is a non-steroidal drug used as an

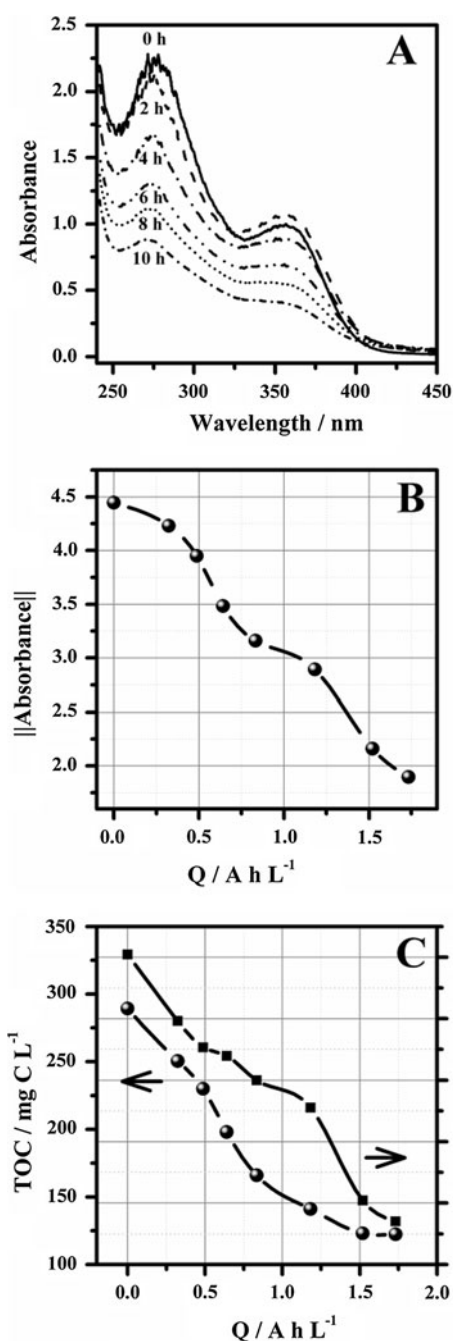


**Fig. 5** Results of electro-degradation mixture of chlortetracycline, oxytetracycline and diclofenac at Na<sub>2</sub>SO<sub>4</sub> solution using Si/BDD anode. **a** UV/Vis spectra obtained during reaction times; **b** Euclidian norm of spectra versus specific charge; **c** TOC and COD analysis

anti-inflammatory, analgesic and anti-pyretic in treatments of human fever and pain, and is considered to be one of the most important pharmaceutical contaminants in wastewater treatment plants [42].

Figure 6a presents the UV/Vis spectra obtained during the process. This result is in accordance with Ciríaco et al. [42], who also found an increase in absorbance in the range

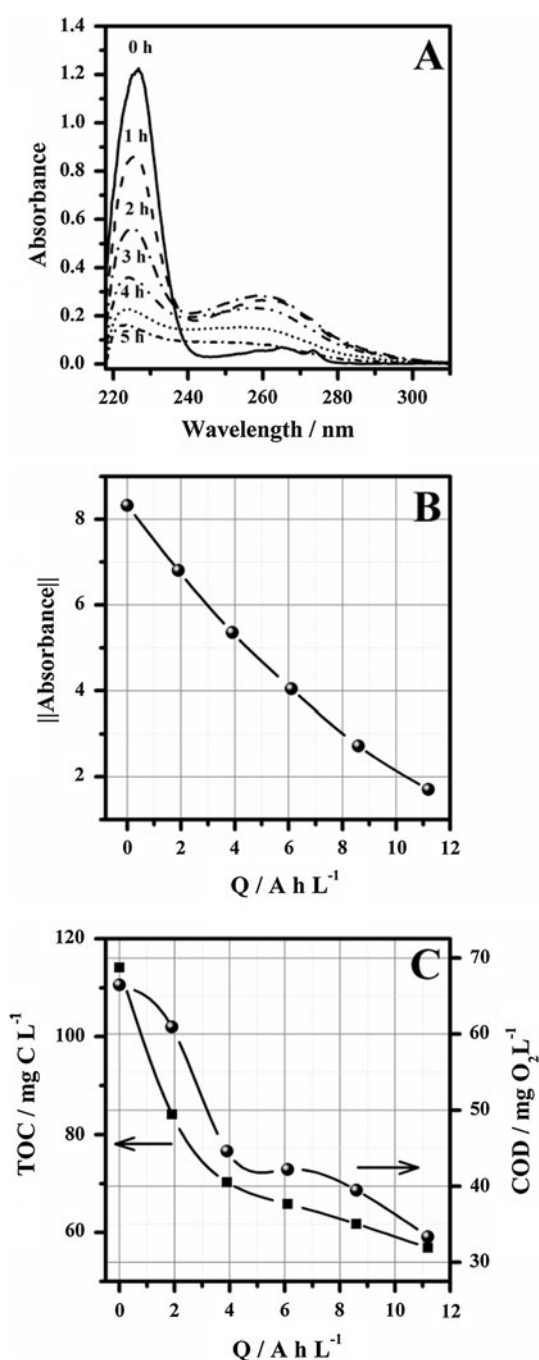


**Fig. 6** Results of electro-degradation of ibuprofen in Na<sub>2</sub>SO<sub>4</sub> solution using Nb/BDD anode. **a** UV/Vis spectra obtained during reaction times; **b** Euclidian norm of spectra versus specific charge; **c** TOC and COD analysis versus specific charge

of 240–300 nm in the initial process. The absorbance norm removal was about 80 %, as shown in Fig. 6b indicating an excellent result.

According to Fig. 6c, the results of organic matter removal monitored using TOC and COD were about 54 and 52 %, respectively. These results were obtained

after  $11.3 \text{ A h L}^{-1}$ , reaching an energy efficiency of  $72.0 \text{ kWh m}^{-3}$ .

Skoumal et al. [43] observed in their studies that ibuprofen is a compound of difficult degradation, due to the formation of highly persistent by-products that decrease the efficiency of the process. Ciríaco et al. [42] obtained 60 % COD removal using  $20 \text{ mA cm}^{-2}$  and Skoumal et al. [43] obtained 92 % COD removal using a combination of AOPs i.e., solar photoelectro-Fenton with BDD. Compared with the literature, our results were wholly satisfactory.

Si/BDD and Nb/BDD electrodes were anodically stable during electrolysis in  $0.1 \text{ mol L}^{-1} \text{ H}_2\text{SO}_4$  at  $30 \text{ mA cm}^{-2}$  for more than 30 and 60 h, respectively. Afterwards, the anodes presented electrochemical instabilities due to film micro-defects, exposing the substrate to the electrolyte, causing delamination and subsequent electrode failure. In the case of the Si/BDD anode, electrical impedance decreased once the doped silicon was a better conductor than the doped diamond. For the Nb/BDD anode, electrical impedance increased due to the formation of resistive and chemically inert carbides.

#### 4 Conclusions

New possibilities for electrochemical cell design are advanced as a promising alternative to conventional plate-shape electrodes. Cylindrical-shape electrodes minimized the physical space required, and were easy to assemble, handle and connect electrically.

BDD films deposited onto Si- and Nb-cylindrical anodes, which were characterised by SEM, Raman spectroscopy and voltammetry. For both substrates, the results indicated adherent polycrystalline films without cracks or delamination, the presence of residual stress, a potential window and electrical conductivity suitable for electrochemical applications.

A solution of ibuprofen and a mixture of chlortetracycline, oxytetracycline and diclofenac were successfully electrolyzed. The monitoring of electro-oxidation was performed employing UV/Vis spectra, COD and TOC. Removal of absorbance, TOC and COD were acceptable for both solutions during the electrochemical degradation. Ibuprofen was recognized as difficult to oxidize, which is in accordance with the literature.

Cylindrical Si/BDD and Nb/BDD electrodes were anodically stable during electrolysis. Cylindrical anodes with adherent boron-doped diamond films are an extremely promising geometric-shape for several electrochemical applications, principally in wastewater treatments.

**Acknowledgments** The electron microscopy study was performed with the SEM-FEG (JEOL6330F) microscope of the LME/LNLS–Campinas. We are grateful to the Companhia Brasileira de Metalurgia

e Mineração (CBMM) for the donation of the niobium used in this study. We also acknowledge the Brazilian agencies CAPES, FAPESP, FAPEMIG, FUNARBE and CNPq for financial support.

#### References

- Schwarzenbach RP, Escher BI, Fenner K, Hofstetter TB, Johnson CA, von Gunten U, Wehrli B Science 313(5790):1072–1077
- Zhu X, Ni J, Wei J, Xing X, Li H (2011) J Hazard Mater 189:127
- Khetan SK, Collins TJ (2007) Chem Rev 107:2319
- Stackelberg PE, Gibs J, Furlong ET, Meyer MT, Zaugg SD, Lippincott RL (2007) Sci Total Environ 377:255
- Oller I, Malato S, Sanchez-Perez JA (2011) Sci Total Environ 409:4141
- Pera-Titus M, Garcia-Molina V, Banos MA, Gimenez J, Esplugas S (2004) Appl Catal B-Environ 47:219
- Rodrigo MA, Canizares P, Buitron C, Saez C (2010) Electrochim Acta 55:8160
- Kapalka A, Foti G, Comninellis C (2009) Electrochimica Acta 54: 2018
- Martinez-Huitle CA, Brillas E (2009) Appl Catal B-Environ 87:105
- Katsaounis A (2010) J Appl Electrochem 40:885
- Palmas S, Polcaro AM, Vacca A, Mascia M, Ferrara F (2007) J Appl Electrochem 37:1357
- Zheng Y, Su W, Chen S, Wu X, Chen X (2011) Chem Eng J 174:304
- Papastefanakis N, Mantzavinos D, Katsaounis A (2010) J Appl Electrochem 40:729
- Sirés I, Brillas E, Cerisola G, Panizza M (2008) J Electroanal Chem 613:151
- Alfaro M, Ferro S, Martinez-Huitle CA, Vong YM (2006) J Brazil Chem Soc 17:227
- Hongna Li, Zhu X, Jinren Ni (2011) Electrochimica Acta 56:9789
- Fryda M, Herrmann D, Schafer L, Klages CP, Perret A, Haenni W, Comninellis C, Gandini D (1999) New Diam Front Carbon Technol 9:229
- Teófilo RF, Ceragioli HJ, Peterlevitz AC, Da Silva LM, Damos FS, Ferreira MMC, Baranauskas V, Kubota LT (2007) J Solid State Electrochem 11:1449
- Rodrigo MA, Canizares P, Sanchez-Carretero A, Saez C (2010) Catal Today 151:173
- Trava-Airoldi VJ, Moro JR, Corat EJ, Goulart EC, Silva AP, Leite NF (1998) Surf Coat Tech 108:437
- Baranauskas V, Ceragioli HJ, Peterlevitz AC (2002) Thin Solid Films 420:151
- Borges C, Pfender E, Heberlein J, Anderson C (1998) Diam Relat Mat 7:1351
- Baranauskas V, Peterlevitz AC, Zanin HG, Teófilo RF, Ceragioli HJ, Kubota LT (2011) World Intellectual Property Organization PCT/BR 2010/000385: 1
- Zanin H, Peterlevitz AC, Ceragioli HJ, Teófilo RF, Degasper FT, Baranauskas V (2012) ECS J Solid State Sci Technol 1:N67
- Li J, Tao T, Li X-b, Zuo J-l, Li T, Lu J, Li S-h, Chen L-z, Xia C-y, Liu Y, Wang Y-l (2009) Desalination 239:139
- Baranauskas V, Ceragioli HJ, Peterlevitz AC (2003) Diam Relat Mat 12:346
- Baranauskas V, Ceragioli HJ, Peterlevitz AC, Durrant SF (2001) Thin Solid Films 398:250
- Fryda M, Matthee T (2009) 12/337 770: 1
- Granger MC, Witek M, Xu JS, Wang J, Hupert M, Hanks A, Koppang MD, Butler JE, Lucazeau G, Mermoux M, Strojek JW, Swain GM (2000) Anal Chem 72:3793
- Mahe E, Devilliers D, Comninellis C (2005) Electrochim Acta 50:2263

31. Chen XM, Chen GH, Gao FR, Yue PL (2003) *Environ Sci Technol* 37:5021
32. Swain G (2004) In: Bard AJ, Rubinstein I (eds) *Electroanalytical chemistry: a series of advances*, vol 22. Marcel Dekker Inc, New York, p 181
33. Kapalka A, Fóti G, Comninellis C (2008) *Electrochem Commun* 10:607
34. Fischer AE, Show Y, Swain GM (2004) *Anal Chem* 76:2553
35. Chaplin BP, Wyle I, Zeng H, Carlisle JA, Farrell J (2011) *J Appl Electrochem* 41:1329
36. Matamoros V, Jover E, Bayona JM (2010) *Anal Chem* 82:699
37. Boyd GR, Reemtsma H, Grimm DA, Mitra S (2003) *Sci Total Environ* 311:135
38. Barnes KK, Kolpin DW, Furlong ET, Zaugg SD, Meyer MT, Barber LB (2008) *Sci Total Environ* 402:192
39. Zhao J-L, Ying G-G, Wang L, Yang J-F, Yang X-B, Yang L-H, Li X (2009) *Sci Total Environ* 407:962
40. Miao X-S, Bishay F, Chen M, Metcalfe CD (2004) *Environ Sci Technol* 38:3533
41. Koutsouba V, Heberer T, Fuhrmann B, Schmidt-Baumler K, Tsipi D, Hiskia A (2003) *Chemosphere* 51:69
42. Ciriaco L, Anjo C, Pacheco MJ, Lopes A, Correia J (2009) *Electrochim Acta* 54:1464
43. Skoumal M, Rodriguez RM, Cabot PL, Centellas F, Garrido JA, Arias C, Brillas E (2009) *Electrochim Acta* 54:2077
44. Zhao X, Qu J, Liu H, Qiang Z, Liu R, Hu C (2009) *Appl Catal B-Environ* 91:539
45. Brillas E, Garcia-Segura S, Skoumal M, Arias C (2010) *Chemosphere* 79:605
46. Ciriaco L, Santos D, Pacheco MJ, Lopes A (2011) *J Appl Electrochem* 41:577
47. Vedenyapina MD, Strel'tsova ED, Davshan NA, Vedenyapina AA (2011) *Russ J Appl Chem* 84:204
48. Zhang H, Liu F, Wu X, Zhang J, Zhang D (2009) *Asia-Pac J Chem Eng* 4:568
49. Rossi A, Alves VA, Da Silva LA, Oliveira MA, Assis DOS, Santos FA, De Miranda RRS (2009) *J Appl Electrochem* 39:329
50. Zhao X, Hou Y, Liu H, Qiang Z, Qu J (2009) *Electrochim Acta* 54:4172